Co-removal of phosphorus and nitrogen with commercial 201 × 7 anion exchange resin during tertiary treatment of WWTP effluent and phosphate recovery

Liang-Liang Wei[a], Guang-Zhi Wang[a], Jun-Qiu Jiang[a], Guo Li[d], Xiao-Lei Zhang[a,c], Qing-Liang Zhao[a,b,]*, Fu-Yi Cui[a,b]

[a]School of Municipal & Environmental Engineering, Harbin Institute of Technology, Harbin 150090, China,
Tel. +86 451 86283008; email: weill333@163.com (L.-L. Wei), Tel. +86 451 86283017; email: hitwgz@126.com (G.-Z. Wang),
Tel. +86 451 86283017; email: jiangjq_hit@126.com (J.-Q. Jiang), Tel. +86 185 63956992; email: 731340455@qq.com (X.-L. Zhang),
Tel/Fax: +86 451 86283017; email: qlzhao@hit.edu.cn (Q.-L. Zhao), Tel. +86 451 86282098; email: cuifuyi@hit.edu.cn (F.-Y. Cui)
[b]State Key Laboratory of Urban Water Resources and Environment (SKLUWRE), Harbin Institute of Technology, Harbin 150090, China
[c]Ship Department, Sunrui Marine Environment Engineering Co., Ltd, Qingdao 266000, China
[d]Key Laboratory of the Three Gorges Reservoir Region's Eco-Environment, Ministry of Education, Chongqing University, Chongqing 400045, China, Tel. +86 186 12858528; email: liguobj@126.com (G. Li)

ABSTRACT

Excessive nitrogen and phosphorus discharge into natural water from wastewater treatment plants still have the potential of causing eutrophication. How to remove those excessive nitrogen and phosphorus in an appropriate way is welcome in practice. This study co-removed nitrate and phosphorus via the operation of commercial 201 × 7 exchange resin column, and recovered phosphate simultaneously. Experimental results demonstrated that the adsorption of PO_4^{3-}-P onto the 201 × 7 resin satisfactorily fitted to Freundlich isotherm, while NO_3^--N followed Langmuir model, with a maximum adsorption capacity of 12.47 mg/g for PO_4^{3-}-P and 107.59 mg/g for NO_3^--N, respectively. Up to 92% of PO_4^{3-}-P and 90% of NO_3^--N in the secondary effluent were recovered by 201 × 7 resin column under the optimal flow rate of 50 BV/h. The exhausted 201 × 7 resin could be regenerated by 5% NaCl within 1 h at a flow rate of 15 BV/h. Moreover, this regeneration would guarantee the effluent PO_4^{3-}-P and NO_3^--N are lower than the breakthrough points even when 1175 BV wastewater passed the resin column. These findings are of great significance for ensuring stricter effluent phosphorus and total nitrogen discharge criteria.

Keywords: Phosphorus recovery; Nitrate removal; Adsorption; Secondary effluent; Ion exchange resin; Regeneration

*Corresponding author.

1. Introduction

Phosphorus and nitrogen are indispensable raw materials used in industry; however, their uncontrolled discharging along with wastewater caused serious eutrophication of aqueous ecosystems [1,2]. For example, the presence of 1 mg/L phosphorus will be sufficient to stimulate algal bloom in lakes, rivers, and reservoirs; thus, the US-EPA has established a maximum contaminant proxy of 0.02 mg/L phosphorus for the enclosed and anoxic lakes [3,4]. Although majority of pollutants in wastewater could be simultaneously removed during biological wastewater treatments [5–7], the nitrogen (mostly as nitrate) and phosphorus (mostly as orthophosphate) from WWTPs effluent are believed to be the main sources of nutrient release into the aquatic environment [8,9]. Meanwhile, nitrate in the secondary effluent is also highly concerned for its potential health threat (e.g. leading to methemoglobinemia of infant) [10,11]. As a result, many countries intend to set the discharge levels of phosphate and total nitrogen to 0.1 and 10 mg/L, or even lower [12–14], and further removal and recovery of nitrogen and phosphorus from the secondary effluent of WWTPs attract many attentions [15,16].

Considering the resource depleting characteristics of phosphorus [5] and the stricter effluent N/P discharge criteria for conventional wastewater treatment plant, how to efficiently and economically remove/recover those phosphorus and nitrate in WWTPs effluent is practically urgent. One of the feasible treatment for reducing nitrogen and phosphorus from wastewater before discharge to aqueous water bodies is to remove their mass flow from the drainage basin [12]. Traditionally, phosphate in wastewater exists as stable state, which has to be removed as solid phosphate materials even after biological wastewater treatment, and accordingly the efficient reduction of phosphate is the rate-limiting step of the co-removal process.

The traditional precipitation-sorption [17–19], crystallization [20], and biological nutrient removal processes [21] are unable to reduce phosphate to a desired low concentration [12,22]. Recently, the usage of ion exchanger is expanding because some polymeric anion exchangers have specific selectivity for phosphate [23,24]. This process has been identified as a feasible alternative for its operational simplicity and adaptability to various wastewater characteristics [25,26]. In addition, the adsorbed phosphate onto the exchange resins can be collected by backwashing, and further precipitated and recovered as calcium phosphate $(Ca_5(PO4)_3OH)$ [17,27]. In order to further enhance the specific selectivity of the resin, polymeric ligand exchanger [28], hybrid anion exchanger (HAIX)

[29], chelating resins [10], iron oxide nanoparticles-embedded anion exchange resin [25] have been applied in recent studies. Although the above-mentioned selective resins are new and highly efficient in removing phosphate [30], the existence of nitrogen within the treated effluent makes it difficult to meet the stricter permissible discharge levels of WWTPs. Moreover, the recent exploring of selective resins has mainly focused on the phosphorus removal rather than nitrate, and seldom mentioned the co-removal of these two pollutants. The commercial macromolecule anion exchange resin could be a better choice for co-removal of phosphorus and nitrate from the secondary effluent of WWTPs, with such advantages as low cost and local availability.

The objective of this work was to realize the co-removal of phosphorus and nitrate present in the secondary effluent of WWTP with the commercial 201×7 anion exchange resin. The main scopes of the study were: (1) to investigate the adsorption capacity and kinetic characteristics of phosphorus and nitrate; (2) to identify the optimal operational conditions of the resin column; (3) to determine the regeneration mode of the resins; and (4) to examine the impacts of regeneration on the recovery of phosphorus and removal of nitrate.

2. Materials and methods

2.1. Commercial anion resin

The strong basic anion exchange resin 201×7 of gel-type (an equivalent to Amberlite IRA-400 in

Table 1
Physical and chemical properties of 201×7 resin

Items	Properties
Unit molecular structure	Styrene-DVB
Type	Strong-base, gel
Function group	$-N^+(CH_3)_3$
Total exchange capacity	≥3.6 mmol/g (dry mass); ≥1.10 mmol/mL (wet mass)
Physical aspect	Pale yellow to golden yellow spherical particles
Granulometry (mm)	0.315–1.25
Humidity (%)	42–48
True density (g/mL)	1.06–1.11
Apparent density (g/mL)	0.66–0.75
Limit of temperature (℃)	OH:40 Cl:100
Limits of pH	1–14
Ionic form	Cl
Referred resins products	Amberlite IRA-400; AB-17; Diaion SA-10A

America), which was an ideal material to adsorb polar compounds in wastewater, was obtained from the Chemical Plant of Nankai University (Tianjin, China). This type of resin was widely used in the adsorption of PO_4^{3-}-P [31], SO_4^{2-}, and NO_3^--N [32–34]. Prior to experiments, the 201×7 resin was firstly pretreated following the standard procedure of cyclic rinse with HCl/NaOH solutions (0.1 M) for two cycles. After air-drying, the resin was dried in vacuum at 40°C for the subsequent tests. Its physical and chemical properties are shown in Table 1.

2.2. Experimental resin column setup and operation

A lab-scale ion exchange column with an effective height of 100 mm was made of Plexiglas ($\phi 24 \times 180$ mm). Both synthetic wastewater and the secondary effluent obtained from a local WWTP were served as the influent of the ion exchange column, with the water quality being summarized in Table 2 (triplicate analysis). The synthetic wastewater was prepared for studying optimal parameters and the actual secondary effluent was for validating the 201×7 resin column efficiencies. Wastewater was pumped upward through the column at a desired velocity controlled by a peristaltic pump during the tests, the effluents at the outlet of resin column were collected at regular time intervals and the PO_4^{3-}-P, NH_4^+-N, NO_3^--N, Cl^-, SO_4^{2-}, and other ions were measured using ion chromatograph (Thermo ICS-5000, USA) in triplicate. In order to further study the breakthrough behaviors and regeneration characteristics of 201×7 resin, different flow rates and varied concentration of NaCl (as regeneration solution) were used in the experiment [10,26] to evaluate the recovery rate of PO_4^{3-}-P and removal efficiency of NO_3^--N.

2.3. Adsorption tests

The effect of experimental parameters including adsorption time (5 min–24 h), initial adsorbent doses

Table 2
Water quality of synthetic wastewater and secondary effluent fed into the ion exchange column

Parameters	Unit	Synthetic wastewater	Secondary effluent
pH	–	7.83	8.23
PO_4^{3-}-P	mg/L	1.2	1.2
COD	mg/L	30.0	30.1
NH_4^+-N	mg/L	4.5	4.2
NO_3^--N	mg/L	20.0	20.4
Cl^-	mg/L	80.0	80.5
SO_4^{2-}	mg/L	30.0	30.4

(1–30 g/L), initial PO_4^{3-}-P (0.3–5.0 mg/L), and NO_3^--N (2.5–50.0 mg/L) concentrations were investigated in batch tests. The initial pH of the solutions was adjusted to 7.0 by adding proper amount of NaOH or HCl before each adsorption. Specifically, the impact of adsorption time on PO_4^{3-}-P removal was studied at pH 7.0 and 298 K (stirred at 150 r/min), and the resin dosage was 100 mg/L. For the adsorbent dosage studies, the adsorption was performed by adding different resin into an aqueous solution containing 1.2 mg/L of PO_4^{3-}-P or 20.0 mg/L of NO_3^--N, shaken (150 r/min) at 298 K for 3 h. Correspondingly, the adsorption kinetics was studied by dosing 200 mg/L of 201×7 resin into an aqueous solution containing different concentrations of PO_4^{3-}-P and NO_3^--N, shaken (150 r/min) at 298 K for varied reaction times.

2.4. Adsorption isotherm and kinetic models

Langmuir and Freundlich isotherms are traditionally employed to describe the thermodynamic adsorptive behavior of different adsorbents. Specifically, Langmuir isotherm assumes that adsorption takes place at specific homogenous sites within the adsorbent, where the sorption of each sorbate molecule onto the surface has equal sorption activation energy, while Freundlich model can apply to multilayer adsorption [35]. A complete discussion on Langmuir and Freundlich models has been described elsewhere and the adsorption isotherms can be described by Eqs. (1) and (2), respectively [36].

$$\frac{1}{Q_e} = \frac{1}{Q_0} + \frac{1}{bQ_0C_e} \tag{1}$$

$$\log Q_e = \log K_F + \frac{1}{n} \log C_e \tag{2}$$

where Q_e is the amount adsorbed (mg/g), C_e is the equilibrium concentration of the adsorbate (mg/L), and Q_0 and b are Langmuir constants related to the maximum adsorption capacity and the energy of adsorption, respectively. Correspondingly, K_F (mg/g) and n are Freundlich constants related to the adsorption capacity and adsorption intensity.

To evaluate the kinetic characteristics of 201×7 resin for PO_4^{3-}-P and NO_3^--N removal, the adsorption kinetics is also described by pseudo-first-order Lagergren equation (Eq. (3)), pseudo-second-order rate equation (Eq. (4)), and the intraparticle diffusion model (Eq. (5)) [37], which can be expressed in their linear forms:

$$\ln(q_e - q_t) = \ln q_e - k_1 t \qquad (3)$$

$$\frac{t}{q_t} = \frac{1}{q_e^2 k_2} + \frac{t}{q_e} \qquad (4)$$

$$q_t = k_i(t^{1/2}) + C \qquad (5)$$

where k_1 (min^{-1}), k_2 (g mg^{-1} min^{-1}), and k_i (mg g^{-1} min$^{-0.5}$) are the rate constants of pseudo-first-order adsorption, pseudo-second-order adsorption, and the intraparticle diffusion, respectively. C is the intercept (mg/g), q_t and q_e are the amount of PO_4^{3-}-P or NO_3^--N adsorbed on adsorbent (mg/g) at equilibrium and at time t, respectively.

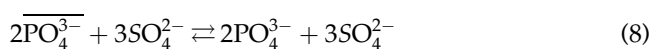### 2.5. Competitive adsorption between PO_4^{3-}-P , Cl^-, NO_3^-, and SO_4^{2-}

The synthetic wastewater with different levels of Cl^-, NO_3^- and SO_4^{2-} (Table 2) was firstly prepared, followed by adding 1.2 mg/L of PO_4^{3-}-P (0.010 M Na$_2$HPO$_4$) into the above-mentioned solutions, then shaken (150 r/min) at 298 K under 200 mg/L resin dosage for 3 h. The selectivity adsorption characteristics of 201 × 7 resin in the presence of anion ions (PO_4^{3-}-P, Cl^-, NO_3^- and SO_4^{2-}) were calculated by comparing the removal efficiency of PO_4^{3-}-P during each adsorption [33].

2.6. Selectivity coefficients

Selectivity coefficient is a dimensionless measure of the relative selectivity between two competing solutes. It is equal to the ratio of the distribution coefficients between the exchanger phase and the aqueous phase [38,39]. According to the Gaines-Thomas convention [40], the selectivity coefficient k_i^j can be expressed as:

$$\overline{PO_4^{3-}} + 3NO_3^- \rightleftarrows PO_4^{3-} + 3\overline{NO_3^-} \qquad (6)$$

$$K_{PO_4^{3-}}^{NO_3^-} = \frac{[PO_4^{3-}] \cdot [\overline{NO_3^-}]^3}{[\overline{PO_4^{3-}}] \cdot [NO_3^-]^3} \qquad (7)$$

$$2\overline{PO_4^{3-}} + 3SO_4^{2-} \rightleftarrows 2PO_4^{3-} + 3\overline{SO_4^{2-}} \qquad (8)$$

$$K_{PO_4^{3-}}^{SO_4^{2-}} = \frac{[PO_4^{3-}]^2 \cdot [\overline{SO_4^{2-}}]^3}{[\overline{PO_4^{3-}}]^2 \cdot [SO_4^{2-}]^3} \qquad (9)$$

$$2\overline{NO_3^-} + SO_4^{2-} \rightleftarrows 2NO_3^- + \overline{SO_4^{2-}} \qquad (10)$$

$$K_{NO_3^-}^{SO_4^{2-}} = \frac{[NO_3^-]^2 \cdot [\overline{SO_4^{2-}}]}{[\overline{NO_3^-}]^2 \cdot [SO_4^{2-}]} \qquad (11)$$

where the barred symbol represents resin-phase anion ions concentrations.

The selectivity of 201 × 7 resin for PO_4^{3-}-P over other anions was determined by shaking 20 mg resin sample with 100 mL solution at pH 7.0 and 298 K, which contained binary mixture of PO_4^{3-}-P and another anion with equal concentrations of 0.05 M [38]. After equilibrium, the concentration of each anion in the supernatant was measured, and equilibrium concentrations of anions in the 201 × 7 resin phase were calculated. Then, the k_i^j for each of the binary system was calculated according to Eqs. (7), (9) and (11).

2.7. Procedure for phosphorus and NaCl recovery from the regenerated eluate

The concentrated NaCl and phosphate in the back-washed eluate from the 201 × 7 resin column were recovered via crystallization and precipitation, respectively [41]. In our experiments, the eluate was firstly evaporated to a 10% volume, and then the crystallized NaCl particles in the concentrated solution were recovered by filtration and drying process. Those recovered NaCl particles were reused for further resin regeneration. Because the solubility of calcium phosphate compounds, such as calcium hydrogen phosphate (Eq. (12)) or hydroxylapatite (Eq. (13)), was limited at a high pH solution, phosphate in the evaporated eluate was directly precipitated and recovered
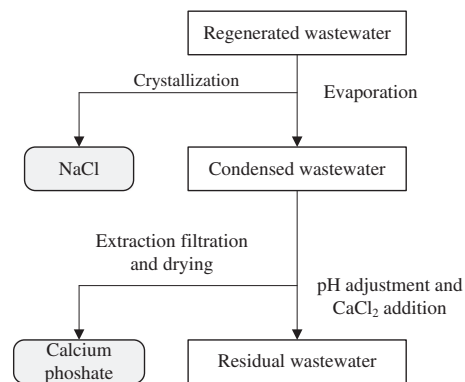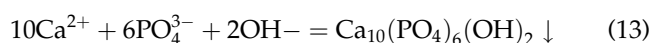

Fig. 1. Phosphorus and NaCl recovery processes during the 201 × 7 resin operation.

as calcium phosphate (Eqs. (12) and (13)) with the addition of 0.1 mol/L CaCl$_2$ solution at pH 10.5 (adjusted by proper amount of 0.1 M NaOH) [9]. The procedure for phosphorus and NaCl recovery is shown in Fig. 1.

$$Ca^{2+} + HPO_4^{2-} = CaHPO_4 \downarrow \tag{12}$$

$$10Ca^{2+} + 6PO_4^{3-} + 2OH- = Ca_{10}(PO_4)_6(OH)_2 \downarrow \tag{13}$$

2.8. Chemical analysis

All chemical parameters (NO$_3^-$-N, PO$_4^{3-}$-P, SO$_4^{2-}$, Cl$^-$, COD, etc.) of the pre- and post-treated wastewater were analyzed according to the Standard Methods [42], and pH was measured by PHS-3C type pH meter (Shanghai Weiye Instrument Plant, China). All measurements were performed in triplicate.

3. Results and discussion

3.1. Phosphate and nitrate adsorption isotherms

The extension of adsorption time (5 min–24 h) and increasing of 201 × 7 resin dosage (10–750 mg/L) enhanced the removal of PO$_4^{3-}$-P and NO$_3^-$-N significantly (Fig. 2(a)), demonstrating that the adsorption would be gradually involved to higher energy sites

once the primary sites were occupied [43]. An adsorption time of 3 h was enough to realize higher PO$_4^{3-}$-P removal efficiency, and thus chosen as the optimal parameter for the subsequent study (Fig. 2(a)). Similarly, a dosage of 200 mg/L resin was optimal because there was a plateau both in PO$_4^{3-}$-P and NO$_3^-$-N sorption isotherms when the dosage exceeded 200 mg/L (Fig. 2(b)).

The equilibrium data for PO$_4^{3-}$-P and NO$_3^-$-N sorption onto 201 × 7 resin (Fig. 2(c) and (d)) showed a nonlinear relationship between resin-phase (Q_e) and solution-phase equilibrium concentrations (C_e), indicating a preferential accumulation of those two pollutant onto 201 × 7 resin [25]. The values of Q_0, b, K_F, n, and the linear regression coefficients for the Langmuir and Freundlich isotherms are summarized in Table 3. Because the Langmuir regression coefficients of NO$_3^-$-N ($R^2 = 0.9626$) were much higher than the corresponding R^2 of Freundlich isotherm (0.8822), it appeared that the monolayer adsorption process of Langmuir model yielded a much better fit than the Freundlich model in simulating the adsorption of NO$_3^-$-N. For comparison, the Freundlich isotherm was slightly fitter than Langmuir model in PO$_4^{3-}$-P adsorption (0.9665 vs. 0.9700), implying a multilayer adsorption of PO$_4^{3-}$-P on the surface of 201 × 7 resin, similar to the previous observation of Sendrowski and Boyer [44] and Tang et al. ($R^2 = 0.9510$) [31]. Based on the Q_0 value obtained from Langmuir isotherm, it might be
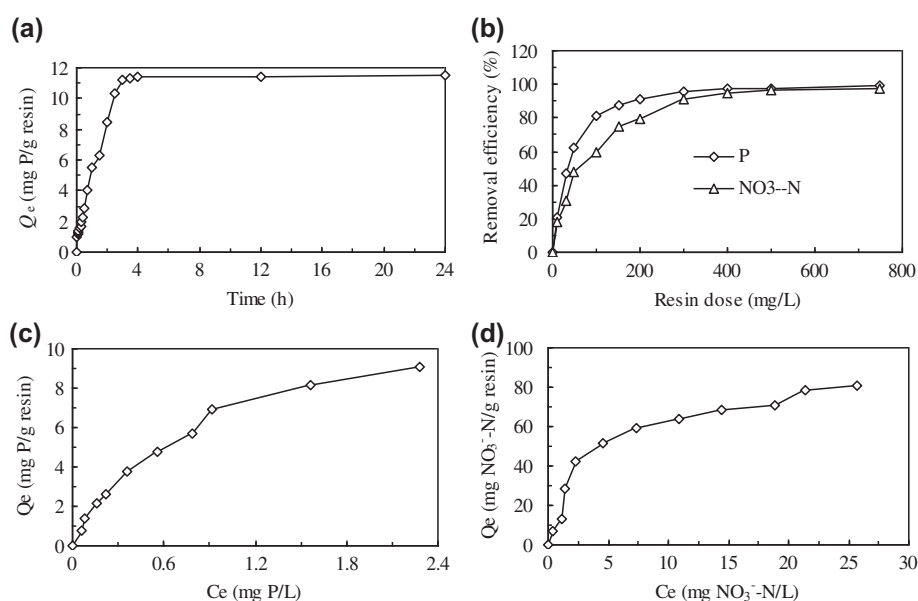

Fig. 2. Experimental data and equilibrium isotherms of 201 × 7 resin adsorption: (a) PO$_4^{3-}$-P removal as a function of adsorption time at 100 mg/L resin dosage, (b) PO$_4^{3-}$-P and NO$_3^-$-N removal as a function of resin dosage, (c) PO$_4^{3-}$-P removal as a function of concentration, and (d) NO$_3^-$-N removal as a function of concentration.

Table 3
Parameters of Langmuir and Freundlich isotherms for the 201 × 7 resin adsorption (calculated from Eqs. (1) and (2)

Adsorbent	Langmuir			Freundlich		
	Q_0 (mg/g)	b	R^2	n	K_F (mg/g)	R^2
PO_4^{3-}-P	12.469	1.265	0.9665	0.663	10.031	0.9700
NO_3^--N	107.590	0.172	0.9626	0.643	90.015	0.8822

concluded that the maximum adsorption capacities (in mg/g) for the 201 × 7 resin were 12.47 for PO_4^{3-}-P and 107.59 for NO_3^--N (Table 3). It should be pointed out that the 201 × 7 resin showed a relatively lower phosphate adsorption capacity than the modified selective resins of HFeO-IRA-400, HZrO-IRA-400, HCuO-IRA-400 [45], FVA fibrous anion exchanger resin [46], and DOW-HFO resin [14], but it was higher than that of the commercial resins of HAIX [26,44], Duolite A-7 [13], D201 × 4, D296, D301R [33], and Purolite A500P [47] resin. In addition, the adsorption of nitrate on the 201 × 7 resin led to similar results with a comparable adsorption capacity of 161.4 mg/g on Amberlite IRA 400 resin [48]. A summary of previously published literatures with the latest important results on the adsorption properties of some resins used for PO_4^{3-} and NO_3^- removal were presented in Table 4.

The pseudo-first-order and pseudo-second-order models were evaluated because of their widespread application to different contaminants, sorbent materials, and water matrices [51]. As shown in Table 5, the second-order kinetic model yielded a much better fit than the first-order adsorption and the intraparticle diffusion in simulating the adsorption processes of PO_4^{3-}-P and NO_3^--N ($R^2 > 0.9638$). Generally, the 201 × 7 resin was more efficient in adsorbing NO_3^--N in comparison with PO_4^{3-}-P, as evidenced by the much lower k_2 value of NO_3^--N (0.009 g mg^{-1} min^{-1}) than PO_4^{3-}-P (0.085 g mg^{-1} min^{-1}). Moreover, the adsorption of NO_3^--N reached equilibrium slowly (>180 min), which could also be described by the intraparticle diffusion model ($R^2 = 0.8460$). Above results were similar to the observation of Malika et al. [52], who found that the late adsorption stage of NO_3^--N by Amberlite IRA 400 resin was well fit to intraparticle diffusion models.

3.2. Effect of competition ions on PO_4^{3-}-P adsorption

The main anions in the secondary effluent of WWTPs are chloride, nitrate, phosphate, and sulfate (Ref. Table 2), and the adsorption capacities of PO_4^{3-}-P in the presence of the competing anions of Cl$^-$, NO_3^--N and SO_4^{2-} are shown in Fig. 3. The adsorption

of PO_4^{3-}-P onto the 201 × 7 resin was strongly affected by the presence of NO_3^--N and SO_4^{2-}, while less affected by Cl$^-$. Specifically, the adsorption efficiency of PO_4^{3-}-P was 52.4% at 80 mg/L Cl$^-$ condition in comparison with the synthetic solution without Cl$^-$ addition. On the other hand, in the presence of 20 mg/L NO_3^--N and 30 mg/L SO_4^{2-}, the removal efficiency of PO_4^{3-}-P was decreased by 53.7% and 69.5%, respectively. This implied that a preferential substitution of PO_4^{3-}-P for SO_4^{2-} over NO_3^--N and Cl$^-$ during the resin adsorption. The above results were similar to the observation that the conventional anion exchange resins had a higher selectivity for sulfate over PO_4^{3-}-P [24,53], and the electrostatic or Coulombic interaction was the underlying mechanism of anion adsorption.

The selectivity coefficients of the 201 × 7 resin for each binary system make the determination of the resin exchanging affinity order possible, and the corresponding binary exchange coefficients of the 201 × 7 resin are given in Table 6. The higher $K_{PO_4^{3-}}^{SO_4^{2-}}$ and $K_{NO_3^-}^{SO_4^{2-}}$ than unity indicated that the 201 × 7 resin had greater SO_4^{2-} affinity than PO_4^{3-}-P, and SO_4^{2-} than NO_3^-. On the contrary, the 201 × 7 resin was proved to be a selective adsorbent for PO_4^{3-}-P over NO_3^-. These results were consistent to the observation of the competition adsorption.

3.3. Factors influencing the performance of ion exchange process

In order to investigate the effect of operational factors on PO_4^{3-}-P and NO_3^--N removal during the 201 × 7 ion exchange column operation, synthetic wastewater was used and such factors as flow rates, concentration of regenerated NaCl solutions, and recycle times were, respectively, examined.

3.3.1. Effect of flow rate on phosphorus and nitrate removal

The effect of flow rates (15, 50, and 80 BV/h) on PO_4^{3-}-P and NO_3^--N removal during resin column operation is shown in Fig. 4. The performance of the 201 × 7 resin column was assessed based on

Table 4
Comparison of different resins on the adsorption of PO_4^{3-} and NO_3^- in wastewater and synthetic solutions

| Resin type	Modification	Contaminants	Experimental conditions	Adsorption capacity (mg/g)	Initial concentration (mg/L)	Fitted model	Reference
Amberlite IRA 400	No	NO_3^-	26℃, pH 6.8, resin dose 2.5 g/L	50.76	2–30	Langmuir ($R^2 = 0.977$)	[49]
	No	NO_3^-	22℃, pH 6.8, resin dose 2.5 g/L	161.4	1–26	Langmuir ($R^2 = 0.982$)	[48]
Amberlite IRA-400 (OH)	No	PO_4^{3-}	21 ± 1℃, pH 1.5–11, resin dose 0.25–4.0 g/L	14.05	10	Freundlich ($R^2 = 0.951$)	[31]
Macroporous anion exchanger (HFO-201)	No	PO_4^{3-}	30℃, pH 6.5–8.0, resin dose 0.5 g/L	17.8	10	Pseudo-first-order ($R^2 = 0.997$)	[50]
Chloride-form anion exchanger Duolite A-7	No	PO_4^{3-}	pH 5.0–7.0, resin dose 2 g/L	4.93	10–300	Langmuir ($R^2 = 0.996$)	[13]
D201×4	No	PO_4^{3-}	pH 6.0–8.5	0.472 (0.496 mg P/mL)	1.23, 5.25 and 10.24	/	[33]
D296	No	PO_4^{3-}	pH 6.0–8.5	0.266 (0.279 mg P/mL)	1.23, 5.25 and 10.24	/	[33]
D301R	No	PO_4^{3-}	pH 6.0–8.5	0.177 (0.186 mg P/mL)	1.23, 5.25 and 10.24	/	[33]
HAIX	No	PO_4^{3-} in WWTP effluent	pH 6.7, resin dosage 0–20 mL/L	0.130 mmol/g	1.8	Freundlich	[26]
HAIX	No	PO_4^{3-} in hydrolyzed urine	pH 9.3, resin dosage 0–450 mL/L	0.164 mmol/g	457	Freundlich	[26]
HAIX	No	PO_4^{3-} in Greywater	pH 7.8, resin dosage 0–20 mL/L	0.126 mmol/g	5.17	Freundlich	[26]
HAIX hybrid anion exchange resin	No	PO_4^{3-} in fresh urine	23℃, pH 6.0, resin dose 50–200 mg/L	9.54	712	/	[44]
HAIX hybrid anion exchange resin	No	PO_4^{3-} in hydrolyzed urine	23℃, pH 9.0, resin dose 50–200 mg/L	7.17	180	Freundlich	[44]
Purolite A500P anion exchange resin	No	PO_4^{3-}	Resin dose 0.5–10 g/L, I 15	7.0	15	/	[47]
Purolite FerrIX A33E resin	No	PO_4^{3-}	24℃, pH 7.2–7.6, resin dose 0.1–1000A0g/L	48	10	/	[9]

(Continued)

Table 4 (*Continued*)

Resin type	Modification	Contaminants	Experimental conditions	Adsorption capacity (mg/g)	Initial concentration (mg/L)	Fitted model	Reference
HFeO-IRA-400	Yes	PO_4^{3-}	22℃	111.1	5	Langmuir ($R^2 = 0.973$)	[45]
HZrO-IRA-400	Yes	PO_4^{3-}	22℃	91.7	5	Langmuir ($R^2 = 0.993$)	[45]
HCuO-IRA-400	Yes	PO_4^{3-}	22℃	74.1	5	Langmuir ($R^2 = 0.977$)	[45]
FVA fibrous anion exchanger	Yes	PO_4^{3-}	30℃, pH 7.0 ± 0.1	32.8–77.2	0.65–50	/	[46]
DOW-HFO (OWEX M4195 resin)	Yes	PO_4^{3-}	20 ± 2℃, pH 8.0, resin dose 0.5–2.0 g/L	23.0	4.25	/	[14]
DOW-HFO-Cu (OWEX M4195 resin)	Yes	PO_4^{3-}	20 ± 2℃, pH 8.0, resin dose 0.5–2.0 g/L	23.0	4.25	/	[14]
201 × 7 resin	No	PO_4^{3-}	25℃, pH 7.0, resin dose 0.01–0.75 mg/L	12.47	0.3–5.0	Freundlich ($R^2 = 0.9700$)	This study
201 × 7 resin	No	NO_3^-	25℃, pH 7.0, resin dose 0.01–0.75 mg/L	107.59	2.5–50.0	Langmuir ($R^2 = 0.9626$)	This study

Table 5
Kinetic parameters of PO_4^{3-}-P and NO_3^--N during the 201 × 7 resin adsorption (calculated from Eqs. 3 to 5)

Adsorbent	C_0 mgL^{-1}	First-order kinetic			Second-order kinetic			Intraparticle diffusion	
		q_e mg g^{-1}	k_1 min^{-1}	R^2	q_e mg g^{-1}	k_2 g mg^{-1} min^{-1}	R^2	k_i mg g^{-1} min$^{-0.5}$	R^2
PO_4^{3-}-P	1.2	11.87	0.389	0.6504	12.195	0.085	0.9638	4.522	0.8178
NO_3^--N	20	112.4	0.299	0.7395	117.647	0.009	0.9792	39.458	0.8460
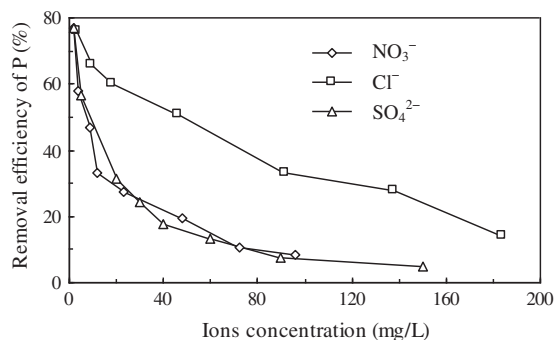
Fig. 3. Effect of competing anions (Cl^-, NO_3^- and SO_4^{2-}) on phosphate adsorption with 201 × 7 ion exchange resin.

breakthrough curves, and the breakthrough point was defined as the bed volumes (BV) of feed provided to the resin column when the effluent PO_4^{3-}-P was 0.3 mg/L and NO_3^--N reached 5.0 mg/L, respectively [26]. Under this definition, the observed breakthrough point was 450 BV at a flow rate of 15 BV/h and 500 BV at 50 BV/h, respectively. As shown in Fig. 4, the flow rate of 15 BV/h would lead to a lower effluent concentration of PO_4^{3-}-P and NO_3^--N, and the concentration of PO_4^{3-}-P still approximated to 0 mg/L when 300 BV synthetic wastewater passed through the resin column. Such a steady removal suggested that the solute diffusion rate of PO_4^{3-}-P onto 201 × 7 resin was a rather rapid process. The initial concentration of PO_4^{3-}-P was 0.40 mg/L under 80 BV/h condition and 0.25 mg/L at 50 BV/h flow rate, much higher than that of 15 BV/h (<0.05 mg/L). Similarly, the initial concentration of NO_3^--N was 1.0, 3.0, and 6.0 mg/L at the condition of 15, 50, and 80 BV/h, respectively. From above, it could be concluded that a larger flow rate led to a higher BV. Generally, the adsorption capacity of 201 × 7 anion exchange resin mainly depended on

Table 6
Selectivity coefficients for the 201 × 7 resin

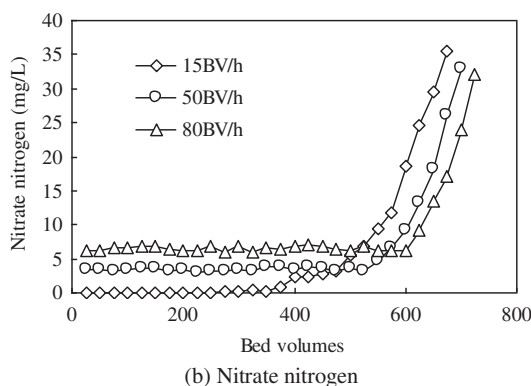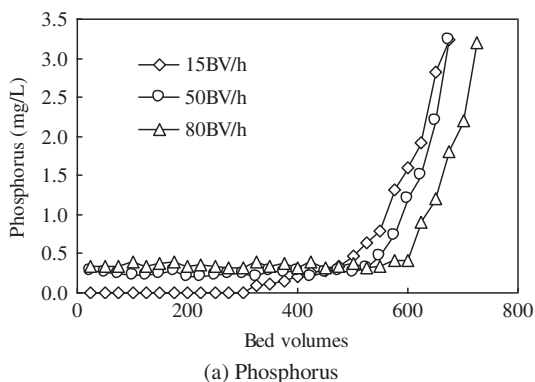|	201 × 7 resin	Standard deviation (%)
$K_{PO_4^{3-}}^{NO_3^-}$	0.87	4.02
$K_{PO_4^{3-}}^{SO_4^{2-}}$	22.27	4.98
$K_{NO_3^-}^{SO_4^{2-}}$	30.26	3.26

(a) Phosphorus

(b) Nitrate nitrogen

Fig. 4. Effect of flow rate on the PO_4^{3-}-P recovery and NO_3^--N removal under different BV.

the content of monofunctional active site of *N*-alkyl [54,55], and the resin columns applied under different conditions had a certain ion exchange capacity [24,33], which might be the main reason for the higher break-through BV at a larger flow rate condition (Fig. 4). Considering the operational cost and the effluent quality, a flow rate of 50 BV/h was chosen in this study. Under this case, more than 0.40 mg PO_4^{3-}-P/g resin and 7.07 mg NO_3^--N/g resin were adsorbed at the breakthrough point. The adsorbed PO_4^{3-}-P/g and NO_3^--N on the resin were much lower than the results obtained from the adsorption tests (Ref. Fig. 2), ascribing to the lack of specific selectivity of the 201 × 7 resin for PO_4^{3-}-P and NO_3^--N in the presence of other competing ions in synthetic wastewater, especially for the existence of SO_4^{2-} [33].

3.3.2. Effect of BV on the removals of ions and COD

Effect of influent BV (50, 100, 150, 200, 250, 300, 350, 400, 450, and 500 BV) on ions removal during resin column operation at a flow rate 50 BV/h is shown in Fig. 5, indicating the removals of PO_4^{3-}-P, NO_3^--N, SO_4^{2-}, and NH_4^+-N, and COD varies widely when the penetrated BV of resin column increased. Briefly, the effluent concentration of NH_4^+-N changed insignificantly when the flow rate increased, with its value almost being equal to that of influent. On the contrary, the breakthrough points of PO_4^{3-}-P and NO_3^--N were 450 BV and 550 BV, respectively. It is noteworthy that the concentration of SO_4^{2-} remained below 0.6 mg/L even when the influent BV reached 600, implying that the 201 × 7 resin showed a remarkable SO_4^{2-} removal. Overall, the following removal sequence was eventually obtained for the 201 × 7 resin: $SO_4^{2-} > PO_4^{3-}$-P $> NO_3^-$-N $>> NH_4^+$, which was similar to the findings demonstrated in previous works [12,25] and the results of the effect of competition anions on PO_4^{3-}-P adsorption.
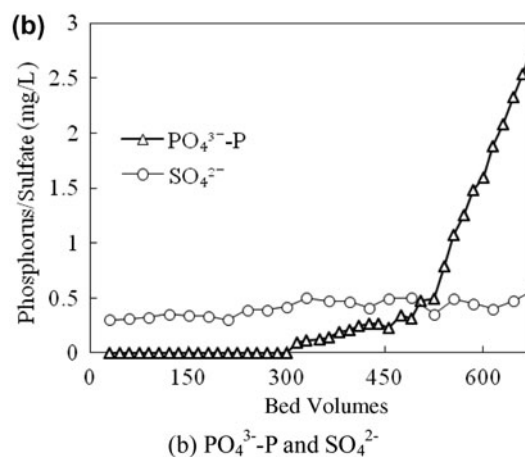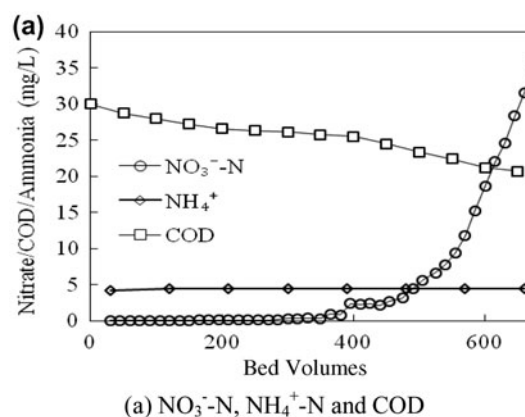

(a) NO_3^--N, NH_4^+-N and COD

(b) PO_4^{3-}-P and SO_4^{2-}

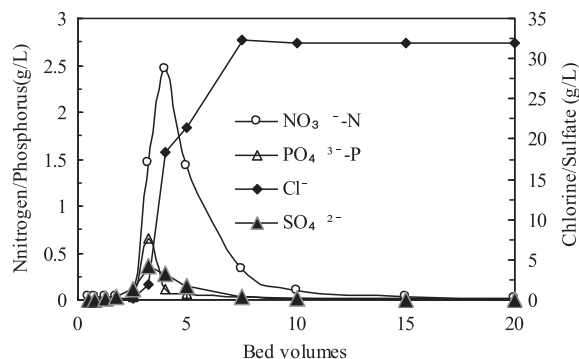Fig. 5. Effluent concentrations of NO_3^--N, NH_4^+-N, COD, PO_4^{3-}-P, and SO_4^{2-} under different BV.

Fig. 6. Regenerated concentration of PO_4^{3-}-P, NO_3^--N, Cl^-, and SO_4^{2-} under different regeneration BV.

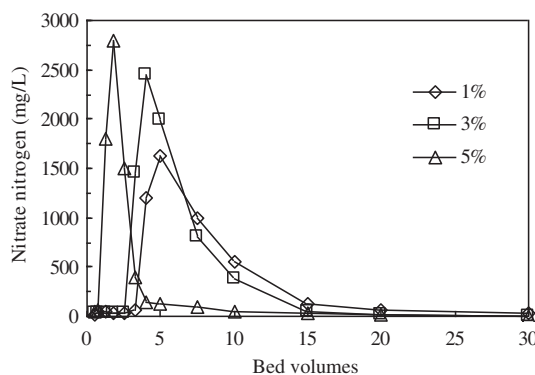### 3.3.3. Effect of resin regeneration on ions removal

Regeneration of the exhausted 201×7 resin is a key process for phosphorus and nitrate removal during resin column operation [25]. Fig. 6 shows the concentration of anions (Cl^-, SO_4^{2-}, PO_4^{3-}-P and NO_3^--N) in the eluate of the exhausted resin backwashed with 3% NaCl (volume of 1, 2, 3, 4, 5, 7.5, 10, 15, and 20 BV). As the regeneration BV of NaCl solution increased, effluent concentrations of SO_4^{2-}, PO_4^{3-}-P, and NO_3^--N exhibited a plateau at approximate 3.5–5.0 BV, and the maximum concentrations of effluent PO_4^{3-}-P and NO_3^--N were 2,676 and 652 mg/L, respectively. The levels of SO_4^{2-}, PO_4^{3-}-P, and NO_3^--N in the backwashing solution dropped sharply when the regenerated NaCl solution increased from 5 to 20 BV. For example, the effluent concentration of PO_4^{3-}-P was 9.7 mg/L at 15 BV condition and was 4.2 mg/L under 20 BV. Above results also implied that an increase of regeneration BV from 15 to 20 was less efficient for NO_3^--N and PO_4^{3-}-P removal; thus, 15 BV was chosen as the optimal BV for the regenerated NaCl solution.

3.3.4. Effect of NaCl concentration for regeneration on ion exchange process

An optimal concentration of the regeneration solution is essential for both phosphate recovery and controlling operational cost; thus, different concentrations of NaCl solution (1, 3, and 5%) were examined for resin column regeneration (Fig. 7). The concentration of NaCl solution would significantly affect (1) the maximum effluent concentration of PO_4^{3-}-P and NO_3^--N in eluates [25], (2) the consumed NaCl volume at maximum effluent PO_4^{3-}-P and NO_3^--N, and (3) the trend of the effluent concentration of PO_4^{3-}-P and NO_3^--N [12]. As shown in Fig. 7, only 2 BV of 5% NaCl solution was sufficient for PO_4^{3-}-P to reach its
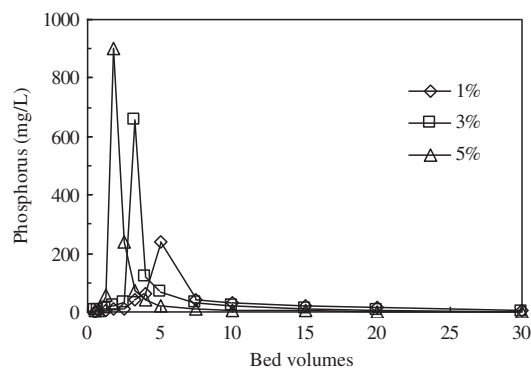
(a) Phosphorus

(b) Nitrate nitrogen

Fig. 7. Effect of NaCl concentration on PO_4^{3-}-P recovery (a) and NO_3^--N removal (b) under different BV.

maximum effluent concentration during the regeneration of resin column, while 5 BV and 3.25 BV for the 3% and 1% NaCl solutions, respectively. Moreover, a higher concentration of NaCl would lead to higher values of the maximal effluent PO_4^{3-}-P and NO_3^--N. Specifically, the maximal PO_4^{3-}-P and NO_3^--N was 910 and 2,819 mg/L when 5% NaCl solution was used, and 652 mg/L PO_4^{3-}-P and 2,676 mg/L NO_3^--N under the condition of 3% NaCl, while only 241 and 2037 mg/L for the 1% NaCl, respectively.

The PO_4^{3-}-P concentration in the eluate after 1 h backwashing by 5% NaCl solution (15 BV/h) was much lower than those of 3% and 1% NaCl solution, with a decreased trend of 3.2 mg/L (5%) < 9.7 mg/L (3%) <21.0 mg/L (1%), indicating that higher NaCl concentration would lead to a better regeneration efficiency. These results were consistent to the previous studies of Nur et al. [9] and Srivastava et al. [56], who found the faster breakthrough of adsorbates and steeper breakthrough at higher filtration velocity. In addition, the concentration profile of PO_4^{3-}-P and NO_3^--N during the elution both exhibited a long tailing, indicating that a relative slower kinetics of the 201×7 resin limited its regeneration efficiency [12].

Table 7
Effect of regenerated NaCl solution on the recovery rate of PO_4^{3-}-P and NO_3^--N

Concentration of NaCl	PO_4^{3-}-P breakthrough point (>0.3 mg/L)	PO_4^{3-}-P regeneration rate (%)	NO_3^--N breakthrough point (>5.0 mg/L)	NO_3^--N regeneration rate (%)
1%	375	75	385	70
3%	450	91	475	87
5%	470	96	495	90

3.3.5. Effect of recycle times of NaCl solution on resin regeneration

Because of the higher selectivity of a monovalent negative anion (Cl⁻ in this case) toward 201 × 7 resin than those ions of higher valences (PO_4^{3-}-P or SO_4^{2-}) and identical valence (NO_3^-) in aqueous-phase electrolyte [33,57], NaCl solution could be recycled for the regeneration of resin column. Meanwhile, the PO_4^{3-}-P and NO_3^--N in the resin column were concentrated within the eluate. The recovery rates of PO_4^{3-}-P and NO_3^--N during the regeneration (15 BV NaCl solution recycled for 1 h) are shown in Table 7. Based on the calculation of eluate PO_4^{3-}-P concentration and the PO_4^{3-}-P retained on the 201 × 7 resin, a recovery rate of 96% for PO_4^{3-}-P was obtained using 5% NaCl, while those of the 3% NaCl and 1% NaCl were decreased to 91 and 75%, respectively. A similar declining trend of NO_3^--N removal was observed and exhibited a general relationship with respect to different NaCl solutions: 5% (90%) >3% (87%) >1% (70%). Obviously, with the increase in NaCl concentration, the exchange capacities of 201 × 7 resin at equilibrium were promoted, ascribing to the generation of ligand strength (or Lewis basicity) at a higher NaCl condition [12,58].

Since a lower breakthrough point of 450 BV was observed for PO_4^{3-}-P in comparison with that of NO_3^--N (550 BV), only the PO_4^{3-}-P regeneration rate
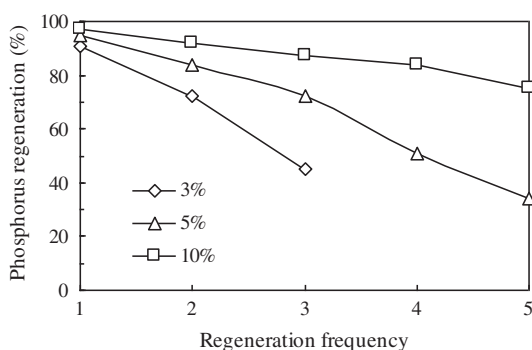

Fig. 8. Regeneration rate of PO_4^{3-}-P vs. cyclic use of NaCl solution.

was analyzed (Fig. 8). The adsorption–desorption process by 3% NaCl solution provided a poor regeneration capacity of the adsorbed PO_4^{3-}-P with larger loss (60%) in its adsorption capacity after three cycles. For comparison, PO_4^{3-}-P recovery rate for the 5% NaCl solution only decreased 22% in the third cycle. Furthermore, the increasing of NaCl concentration to 10% would significantly enhance the recovery process, with more than 75% of PO_4^{3-}-P being recovered even after fifth times of recycling. Considering both regeneration efficiency and operational cost, a solution of 5% NaCl was chosen as an inexpensive regenerant for the exhausted 201 × 7 resin. In addition, no loss of 201 × 7 resin occurred during the adsorption/desorption cycles, indicating its suitability for the recovery of PO_4^{3-}-P and removal of NO_3^--N.

3.4. Efficiency of 201 × 7 resin exchange for secondary effluent treatment

In order to evaluate the practical PO_4^{3-}-P removal/recovery and NO_3^--N removal efficiencies of 201 × 7 resin column, the secondary effluent (Ref. Table 2) was fed into the column with the experimental results being shown in Table 8.

As shown in Table 8, near 1,175 BV volume of tertiary-treated effluent could be produced in the presence of relatively high organic carbon (COD = 30.1 mg/L) after three times regeneration by 5% NaCl solution, achieving an adsorption capacity of 1.04 mg P/g and 18.53 mg N/g [59]. Despite a lower breakthrough adsorption capacity than that of Nur et al. [9], who observed a 4.1 mg P/g breakthrough adsorption capacity during the iron oxide-impregnated strong base anion exchange resin column operation under 5 mg/L phosphate concentration, the characteristics of synchronous removal of NO_3^--N and a low production cost (about 2 dollar/kg) were still meaningful for 201 × 7 resin in practice. Moreover, only 15 BV NaCl was consumed for the regeneration of the resin column. It is worth mentioning that the 201 × 7 resin exchange system is not only highly efficient, but also produce less waste in comparison with the previous

Table 8
The simulated operational process for secondary effluent treatment by 201 × 7 resin exchange

Processes	Parameters	Values or description
Exchange Process 1	Flow rate (BV/h)	50
	Operational time (h)	8
	Volume of wastewater (BV)	400
Regeneration	Regenerated NaCl (%) and flow rate (BV/h)	5%, 15
Process 1	Operational time (h)	1
	Volume of NaCl (BV)	15
Exchange	Flow rate (BV/h)	50
Process 2	Operational time (h)	7
	Volume of wastewater (BV)	350
Regeneration	Regenerated NaCl and flow rate	Regenerated NaCl from process 1
Process 2	Operational time (h)	1
	Volume of NaCl (BV)	15
Exchange	Flow rate (BV/h)	15
Process 3	Operational time (h)	5.5
	Volume of wastewater (BV)	275
Regeneration	Regenerated NaCl and flow rate	Regenerated NaCl from process 2
Process 3	Operational time (h)	1
	Volume of NaCl (BV)	15
Exchange	Flow rate (BV/h)	50
Process 4	Operational time (h)	3
	Volume of wastewater (BV)	150

studies [9,10]. For example, Nur et al. [9] found that only 70% of the phosphate which adsorbed on the iron oxide-impregnated Type II hybrid anion exchange resin could be desorbed by 14 BV NaOH (1.0 M), and 90–95% of the phosphate was recovered by 42 BV NaOH.

Although the anion exchange resins with *N*-alkyl groups might be degraded in alkaline solution under long time operation, however, the exhausted 201 × 7 resin regenerated by 5% NaCl and 1 M NaOH solution showed no noticeable loss in capacity. Thus, the using of 201 × 7 resin could efficiently remove the PO_4^{3-}-P and NO_3^--N from the secondary effluent with high flow rate and economical regeneration.

3.5. Phosphate and NaCl recovery from the regenerated solution

The quality of the eluate produced during regeneration is summarized in Table 9. The concentrations of PO_4^{3-}-P, NO_3^--N and SO_4^{2-} in the recycled NaCl solution were 72.5 mg/L, 1160.2 mg/L, and 2110.5 mg/L, respectively, indicating a characteristic of high salt and low organics. Since the concentrations of PO_4^{3-}-P, NO_3^--N were relatively lower than that of Cl^-, the collected NaCl solution could be evaporated to a 10% volume for NaCl crystallization and separation with 0.45 μm membrane filtration. After evaporation, the concentration of PO_4^{3-}-P and NO_3^--N in the condensed solution reached 710.5 mg/L and 11345.4 mg/L, and the PO_4^{3-}-P could be extracted via calcium phosphate precipitation (optimal condition was pH of 10.5 and Ca/P ratio of 1.67). Under these conditions, more than 92% of the phosphate in the condensed solution could be recovered. Furthermore, the anion ratio of $Cl^-:NO_3^-:SO_4^{2-}$ in the regenerated NaCl solution after the recovery of NaCl and PO_4^{3-}-P was 100:4:2, implying it could be reused in the subsequent resin column regeneration.

3.6. Perspectives of co-removal phosphorus and nitrogen with 201 × 7 resin

Based on the above experimental results, a majority of phosphorus and nitrogen in the secondary effluent was removed by commercial 201 × 7 resin, and 92% of phosphate was further recovered as calcium phosphate.

Assuming a wastewater treatment plant with a design capacity of 10,000 m³/d, with an effluent PO_4^{3-}-P and NO_3^--N of 0.9 mg/L and 15.0 mg/L, the greatest potential for PO_4^{3-}-P recovery is 6 kg/d and for NO_3^--N removal is 100 kg/d using the 201 × 7 ion exchange resin. Only 8.5 m³ commercial 201 × 7 ion exchange resin is needed for constructing the ion exchange system with a 130 m³ volume of 5% NaCl regeneration solution. It is known to all that more than 80% of the soluble phosphorus in the sewage wastewater was converted to solid phase minerals by spontaneous precipitation throughout the biological treatment process [60,61]. Based on this, the using of 201 × 7 ion exchange resin will decrease about another 14% discharge of the phosphorus and

Table 9
Water quality of the recycle used NaCl solution during 201 × 7 resin exchange process

	pH	COD (mg/L)	PO_4^{3-}-P (mg/L)	NO_3^--N (mg/L)	Cl^- (mg/L)	SO_4^{2-} (mg/L)
15 BV	7.54	100.12	72.5	1,160.2	20,650.9	21,10.5

nitrogen in secondary effluent from WWTP. Moreover, this process shows a much lower operational cost as compared to the nanofiltration and reverse osmosis [62], and the exhausted 201×7 resin can be regenerated with no remarkable loss in ion exchange capacity.

4. Conclusion

The following conclusions are drawn based on the above experimental results:

(1) The adsorption of PO_4^{3-}-P onto the 201×7 resin satisfactorily fitted to Freundlich isotherm, while NO_3^--N followed Langmuir model, with maximum adsorption capacities of 12.47 mg/g for PO_4^{3-}-P and 107.59 mg/g for NO_3^--N, respectively.

(2) The 201×7 resin exchange column could be applied to remove PO_4^{3-}-P and NO_3^--N from the secondary effluent simultaneously, the removal of ions showed a decreased trend of $SO_4^{2-} > PO_4^{3-}$-P $> NO_3^-$-N $>> NH_4^+$.

(3) Optimal operational parameters of the 201×7 resin exchange column was 50 BV/h of flow rate, 5% NaCl solution for regeneration under 15 BV/h of flow rate (15 BV). After three times of regenerations, 1,175 BV of secondary effluent was totally treated, with the final effluent concentration of PO_4^{3-}-P and NO_3^--N lower than 0.3 mg/L and 5.0 mg/L, respectively.

(4) The condensed NaCl within the regeneration solution could be crystallized and recovered, and 92% of the condensed PO_4^{3-}-P was recovered via calcium phosphate precipitation. The optimal condition of the calcium phosphate precipitation was pH of 10.5, and Ca/P ration of 1.67.

Acknowledgment

References

[1] D.J. Jeon, S.H. Yeom, Recycling wasted biomaterial, crab shells, as an adsorbent for the removal of high concentration of phosphate, Bioresour. Technol. 100(9) (2009) 2646–2649.

[2] R. Saad, K. Belkacemi, S. Hamoudi, Adsorption of phosphate and nitrate anions on ammonium-functionalized MCM-48: Effects of experimental conditions, J. Colloid Interf. Sci. 311(2) (2007) 375–381.

[3] USEPA (US Environmental Protection Agency), Nutrient criteria technical guidance manual: lakes and reservoirs. EPA-822-B00-001, Office of Water, US Environmental Protection Agency, Washington, DC, 2000.

[4] W. Chouyyok, R.J. Wiacek, K. Pattamakomsan, T. Sangvanich, R.M. Grudzien, G.E. Fryxell, Phosphate removal by anion binding on functionalized nanoporous sorbents, Environ. Sci. Technol. 44(8) (2010) 3073–3078.

[5] Z.G. Liu, Q.L. Zhao, L.L. Wei, D.L. Wu, L.M. Ma, Effect of struvite seed crystal on MAP crystallization, J Chem. Technol. Biot. 86(11) (2011) 1394–1398.

[6] Z.W. Wang, Z.C. Wu, Distribution and transformation of molecular weight of organic matters in membrane bioreactor and conventional activated sludge process, Chem. Eng. J. 150 (2009) 396–402.

[7] L.L. Wei, K. Wang, Q.L. Zhao, C.M. Xie, Characterization and transformation of dissolved organic matter in a full-scale wastewater treatment plant in Harbin, China. Desalin. Water Treat. 46 (2012) 295–303.

[8] R.S.S. Wu, K.H. Lam, J.M.N. Lee, T.C. Lau, Removal of phosphate from water by a highly selective La(III)-chelex resin, Chemosphere 69(2) (2007) 289–294.

[9] T. Nur, M.A.H. Johir, P. Loganathan, T. Nguyen, S. Vigneswaran, J. Kandasamy, Phosphate removal from water using an iron oxide impregnated strong base anion exchange resin, J. Ind. Eng. Chem. 20 (2013) 1301–1307.

[10] P. Loganathan, S. Vigneswaran, J. Kandasamy, Enhanced removal of nitrate from water using surface modification of adsorbents—A review, J Environ. Manage. 131(15) (2013) 363–374.

[11] M.F. Abou Taleb, G.A. Mahmoud, S.M. Elsigeny, S.A. Hegazy. Adsorption and desorption of phosphate and nitrate ions using quaternary (polypropylene-g-N,N-dimethylamino ethylmethacrylate) graft copolymer, J. Hazard. Mater. 159(2–3) (2008) 372–379.

[12] W.D. Henry, D.Y. Zhao, A.K. SenGupta, C. Lange, Preparation and characterization of a new class of polymeric ligand exchangers for selective removal of trace contaminants from water, React. Funct. Polym. 60 (2004) 109–120.

[13] T.S. Anirudhan, B.F. Noeline, D.M. Manohar, Phosphate removal from wastewaters using a weak anion exchanger prepared from a lignocellulosic residue, Environ. Sci. Technol. 40(8) (2006) 2740–2745.

[14] S. Sengupta, A. Pandit, Selective removal of phosphorus from wastewater combined with its recovery as a solid-phase fertilizer, Water Res. 45 (2011) 3318–3330.

[15] X. Zhu, A. Jyo, Column-mode phosphate removal by a novel highly selective adsorbent, Water Res. 39(11) (2005) 2301–2308.

[16] A. Bermúdez-Couso, D. Fernández-Calviño, M.A. Álvarez-Enjo, J. Simal-Gándara, J.C. Nóvoa-Muñoz, M. Arias-Estévez, Pollution of surface waters by metalaxyl and nitrate from non-point sources, Sci. Total Environ. 461–462(1) (2013) 282–289.

[17] L.E. de-Bashan, Y. Bashan, Recent advances in removing phosphorus from wastewater and its future use as fertilizer (1997–2003), Water Res. 38 (2004) 4222–4246.

[18] Z. Bradford-Hartke, P. Lant, G. Leslie, Phosphorus recovery from centralised municipal water recycling plants, Chem. Eng. Res. Des. 90 (2012) 78–85.

[19] J.H. Park, D. Jung, Removal of total phosphorus (TP) from municipal wastewater using loess, Desalination 269 (2011) 104–110.

[20] P. Battistoni, A. De Angelis, P. Pavan, M. Prisciandaro, F. Cecchi, Phosphorus removal from a real anaerobic supernatant by struvite crystallization, Water Res. 35 (2001) 2167–2178.

[21] J. Diaz, E. Ingall, C. Benitez-Nelson, D. Paterson, M. de Jonge, I. McNulty, J.A. Brandes, Marine polyphosphate: a key player in geologic phosphorus sequestration, Science 320 (2008) 652–655.

[22] D. Jenkins, J.F. Ferguson, A.B. Menar, Chemical processes for phosphate removal, Water Res. 5 (7) (1971) 369–389.

[23] B. Saha, S. Chakraborty, G. Das, A mechanistic insight into enhanced and selective phosphate adsorption on a coated carboxylated surface, J Colloid Interf Sci. 331 (2009) 21–26.

[24] Md.R. Awual, A. Jyo, Assessing of phosphorus removal by polymeric anion exchangers, Desalination 281 (2011) 111–117.

[25] L.M. Blaney, S. Cinar, A.K. SenGupta, Hybrid anion exchanger for trace phosphate removal from water and wastewater, Water Res. 41 (2007) 1603–1613.

[26] J.A. O'Neal, T.H. Boyer, Phosphate recovery using hybrid anion exchange: Applications to source-separated urine and combined wastewater streams, Water Res. 47 (2013) 5003–5017.

[27] W.G. Yi, K.V. Lo, Phosphate recovery from greenhouse wastewater, J. Environ. Sci. Heal. B 38 (2003) 501–509.

[28] M. Kumar, M. Badruzzaman, S. Adham, J. Oppenheimer, Beneficial phosphate recovery from reverse osmosis (RO) concentrate of an integrated membrane system using polymeric ligand exchanger (PLE), Water Res. 41 (2007) 2211–2219.

[29] T.H. Boyer, A. Persaud, P. Banerjee, P. Palomino, Comparison of low-cost and engineered materials for phosphorus removal from organic-rich surface water, Water Res. 45 (2011) 4803–4814.

[30] W. Xiong, J. Peng, Development and characterization of ferrihydrite-modified diatomite as a phosphorus adsorbent, Water Res. 42 (19) (2008) 4869–4877.

[31] X.H. Tang, Z. Berner, P. Khelashvili, S. Norra, Preparative separation of arsenate from phosphate by IRA-400 (OH) for oxygen isotopic work, Talanta 105 (2013) 46–51.

[32] Z.Y. Tao, H.M. Zhou, Binary and ternary ion-exchange equilibria- SO42–Cl–NO3–201×7 system, Desalination 69 (1988) 125–134.

[33] S.K. Zheng, J.J. Chen, X.M. Jiang, X.F. Li, A comprehensive assessment on commercially available standard anion resins for tertiary treatment of municipal wastewater, Chem. Eng. J. 169 (2011) 194–199.

[34] Z.W. Zhao, F. Hu, Y.J. Hu, S.B. Wang, P.M. Sun, G.S. Huo, H.G. Li, Adsorption behaviour of WO_4^{2-} onto 201×7 resin in highly concentrated tungstate solutions, Int. J. Refract. Met. H 28 (2010) 633–637.

[35] K.Y. Foo, B.H. Hameed, Insights into the modeling of adsorption isotherm systems, Chem. Eng. J. 156 (2010) 2–10.

[36] L.L. Wei, K. Wang, Q.L. Zhao, C.M. Xie, W. Qiu, T. Jia, Kinetics and equilibrium of adsorption of dissolved organic matter fractions from secondary effluent by fly ash, J Environ. Sci.-China 23 (2011) 1057–1065.

[37] S.B. Wang, Q. Ma, Z.H. Zhu, Characteristics of coal fly ash and adsorption application, Fuel 87(15–16) (2008) 3469–3473.

[38] C.H. Hannachi, F. Guesmi, B. Hamrouni, Study of the ion exchange equilibrium of Cl^-, NO_3^-, and SO_4^{2-} ions on the AMX membrane, Ionics 19 (2013) 329–334.

[39] A. Marton, H. Sakashita, Y. Miura, E. Hiramatsu, Y. Miyazaki, Study of ion exchange selectivity of organic ions by using ^{31}P NMR spectroscopy, Talanta 59 (2003) 217–227.

[40] G.L. Gaines, H.C. Thomas, Adsorption studies on clay minerals. II. A formulation of the thermodynamics of exchange adsorption, J. Chem. Phys. 21 (1953) 714–718.

[41] K.M. Udert, T.A. Larsen, W. Gujer, Estimating the precipitation potential in urine-collecting systems, Water Res. 37 (2003) 2667–2677.

[42] APHA, AWWA, WEF, Standard Methods for the Examination of Water and Wastewater, twenty-first ed., American Public Health Association, Washington, DC, 2005.

[43] M. Ahmaruzzaman, A review on the utilization of fly ash, Prog. Energ. Combust. 36 (2010) 327–363.

[44] A. Sendrowski, T.H. Boyer, Phosphate removal from urine using hybrid anion exchange resin, Desalination 322 (2013) 104–112.

[45] N.Y. Acelas, B.D. Martin, D. López, B. Jefferson, Selective removal of phosphate from wastewater using hydrated metal oxides dispersed within anionic exchange media, Chemosphere (2014) Available from: http://dx.doi.org/10.1016/j.chemosphere.2014.02.024.

[46] Md.R. Awual, A. Jyo, S.A. El-Safty, M. Tamada, N. Seko, A weak-base fibrous anion exchanger effective for rapid phosphate removal from water, J. Hazard. Mater. 188 (2011) 164–171.

[47] B.D. Martin, S.A. Parsons, B. Jefferson, Removal and recovery of phosphate from municipal wastewaters using a polymeric anion exchanger bound with hydrated ferric oxide nanoparticles, Water Sci. Technol. 60 (2009) 2637–2645.

[48] M. Chabani, A. Amrane, A. Bensmaili, Equilibrium sorption isotherms for nitrate on resin Amberlite IRA 400, J Hazard. Mater. 165 (2009) 27–33.

[49] M. Chabani, A. Amrane, A. Bensmaili, Kinetics of nitrates adsorption on Amberlite IRA 400 resin, Desalination 206 (2007) 560–567.

[50] B.J. Pan, J. Wu, B.C. Pan, L. Lv, W.M. Zhang, L.L. Xiao, X.S. Wang, X.C. Tao, S.R. Zheng, Development of polymer-based nanosized hydrated ferric oxides (HFOs) for enhanced phosphate removal from waste effluents, Water. Res. 43 (2009) 4421–4429.

[51] Y.S. Ho, G. McKay, Pseudo-second order model for sorption processes, Process Biochem. 34 (1999) 451–465.

[52] C. Malika, A. Kenza, A.O. Yasmine, A. Abdeltif, B. Aicha, Removal of nitrate from drinking water by adsorption using ion exchange resin, Desalin. Water Treat. 24 (2010) 109–116.

[53] J. Gregory, R.V. Dhond, Anion exchange equilibria involving phosphate, sulphate, and chloride, Water Res. 6 (1972) 695–702.

[54] L.L. Zhu, L. Guo, Z.J. Zhang, J. Chen, S.M. Zhang, The preparation of supported ionic liquids (SILs) and their application in rare metals separation, Sci. China Chem. 55 (2012) 1479–1487.

[55] J.O. Agbenin, C.A. De Abreu, B. van Raij, Extraction of phytoavailable trace metals from tropical soils by mixed ion exchange resin modified with inorganic and organic ligands, Sci. Total Environ. 227 (1999) 187–196.

[56] V.C. Srivastava, B. Prasad, I.M. Mishra, I.D. Mail, M.M. Swamy, Prediction of breakthrough curves for sorptive removal of phenol by bagasse fly ash packed bed, J. Ind. Eng. Chem. 47 (2008) 1603–1613.

[57] D.Y. Zhao, A.K. Sengupta, Ultimate removal of phosphate from wastewater using a new class of polymeric ion exchangers, Water Res. 32 (1998) 1613–1625.

[58] D. Zhao, A.K. SenGupta, Ligand separation with a copper(II)-loaded polymeric ligand exchange, Ind. Eng. Chem. Res. 39 (2000) 455–462.

[59] Md.R. Awual, S.A. El-Safty, A. Jyo, Removal of trace arsenic(V) and phosphate from water by a highly selective ligand exchange adsorbent, J Environ. Sci. -China 23 (12) (2011) 1947–1954.

[60] J. Houhou, B.S. Lartiges, A. Hofmann, G. Frappier, J. Ghanbaja, A. Temgoua, Phosphate dynamics in an urban sewer: A case study of Nancy, France, Water Res. 43(4) (2009) 1088–1100.

[61] G. Bitton, Wastewater Microbiology, fourth ed., Wiley Blackwell, Hoboken, NJ, 2011.

[62] Z. Bradford-Hartke, P. Lant, G. Leslie, Phosphorus recovery from centralised municipal water recycling plants, Chem. Eng. Res. Des. 90 (2012) 78–85.